Molecular Machines Hot Paper

Deutsche Ausgabe: DOI: 10.1002/ange.201509813
Internationale Ausgabe: DOI: 10.1002/anie.201509813

Hierarchical Self-Assembly of Supramolecular Muscle-Like Fibers

*Antoine Goujon[+], Guangyan Du[+], Emilie Moulin, Gad Fuks, Mounir Maaloum, Eric Buhler, and Nicolas Giuseppone**

Abstract: *An acid–base switchable [c2]daisy chain rotaxane terminated with two 2,6-diacetylamino pyridine units has been self-assembled with a bis(uracil) linker. The complementary hydrogen-bond recognition patterns, together with lateral van der Waals aggregations, result in the hierarchical formation of unidimensional supramolecular polymers associated in bundles of muscle-like fibers. Microscopic and scattering techniques reveal that the mesoscopic structure of these bundles depends on the extended or contracted states that the rotaxanes show within individual polymer chains. The observed local dynamics span over several length scales because of a combination of supramolecular and mechanical bonds. This work illustrates the possibility to modify the hierarchical mesoscopic structuring of large polymeric systems by the integrated actuation of individual molecular machines.*

Biomolecular machines are key elements of living organisms that perform essential functions such as replication, synthesis, transport, and motion.[1,2] Among several important characteristics, some of these processes involve the integration of molecular machines in order to amplify their motions at a scale larger than their typical individual size. A well-known example is related to the collective molecular motion produced in muscular tissues because of their hierarchical organization. Within sarcomeres, the coordinated movements of thousands of myosin heads lead to the gliding of thick myosin filaments along thin actin filaments. By polymerizing these contractile sarcomere units longitudinally in myofibrils and by associating these myofibrils laterally in bundled fibers, macroscopic motions can be reached.[3] It thus appears very attractive to take inspiration from these biological processes in order to design artificial systems displaying such a hierarchical structuring for the amplification of molecular motions and for their implementation in nanotechnology and materials science.[4–6]

The group of Sauvage reported in 2000 the first bioinspired molecular muscle based on a bistable [*c*2]daisy chain rotaxane incorporating two coordination stations on its axle. This individual machine can achieve a switchable contraction/extension motion with an amplitude of 1.8 nm depending on the nature of the coordinated metal ions (Cu^{I} or Zn^{II}).[7] Although a number of rotaxane-based molecular muscles was subsequently developed,[4a] their integration within oligomers and polymers was only recently envisioned to access artificial muscle-like materials.[8–11] Our group described the first amplification of such molecular motions up to the microscopic scale by linking thousands of bistable rotaxanes within single-chain polymers.[10] However, in order to build contractile materials from molecular machines, further hierarchical organization of these single-chain polymers into higher-scale structures is required, as myofibrils do when laterally packed in bundles of muscular fibers.[4b] Here we show that such a hierarchical structuring is possible within a system incorporating supramolecular polymers based on hydrogen-bonded [*c*2]daisy chain rotaxanes.

Multiple hydrogen-bond motifs have been described for the preparation of supramolecular polymers because of their high directionality, kinetic lability, and ease of synthesis.[12,13] For instance, Lehn and co-workers implemented the uracil:diaminopyridine recognition pattern to produce chiral triple helices at the micrometric scale with liquid-crystalline properties.[14,15] This heterocomplementary motif was then used to produce a variety of morphologies (spheres, rods, fibers) with a controlled degree of polymerization.[16]

Inspired by this hydrogen-bond polymerization unit, and in a continuation of our initial reports,[10,17] we targeted the synthesis of [*c*2]daisy chain rotaxane (**12**) with two diacetylamino pyridine units as stoppers, and a complementary ditopic linker (**5**) incorporating two 1-hexyluracil moieties at its extremities (Scheme 1). Molecule **5** was also decorated with branched alkyl chains to ensure solubility in organic solvents[18,19] and to provide additional van der Waals interactions for stabilizing the primary hydrogen-bond pattern in a cooperative self-assembly. We also envisioned that a mismatch between the polar character of rotaxane unit **12** (presence of crown ethers and ion pairs) and the apolar character of linker **5**, would favor lateral aggregations of the single-chain supramolecular polymers driven by microphase separation, thus reinforcing the cooperative mechanism of the supramolecular polymerization.

Bis(uracil) linker **5** was synthesized in five steps using Sonogashira couplings as key reactions (Scheme 1 a). Initially, branched alkyl bromide **1**, prepared from commercially available 2-hexyl-1-decanol using the Appel reaction, was

[*] A. Goujon,[+] Dr. G. Du,[+] Dr. E. Moulin, Dr. G. Fuks, Prof. Dr. M. Maaloum, Prof. Dr. N. Giuseppone
SAMS research group, Institut Charles Sadron, CNRS
University of Strasbourg
23 rue du Loess, BP 84047, 67034 Strasbourg Cedex 2 (France)
E-mail: giuseppone@unistra.fr
Prof. Dr. E. Buhler
Matière et Systèmes Complexes (MSC) Laboratory
University of Paris Diderot—Paris VII, UMR 7057
Bâtiment Condorcet, 75205 Paris Cedex 13 (France)
Dr. G. Du[+]
Current address:
Southwest Petroleum University, No.8 Xindu Avenue
Xindu District, Chengdu City, Sichuan Province 610500 (P.R. China)
[+] These authors contributed equally to the work.

Supporting information for this article is available on the WWW under http://dx.doi.org/10.1002/anie.201509813.

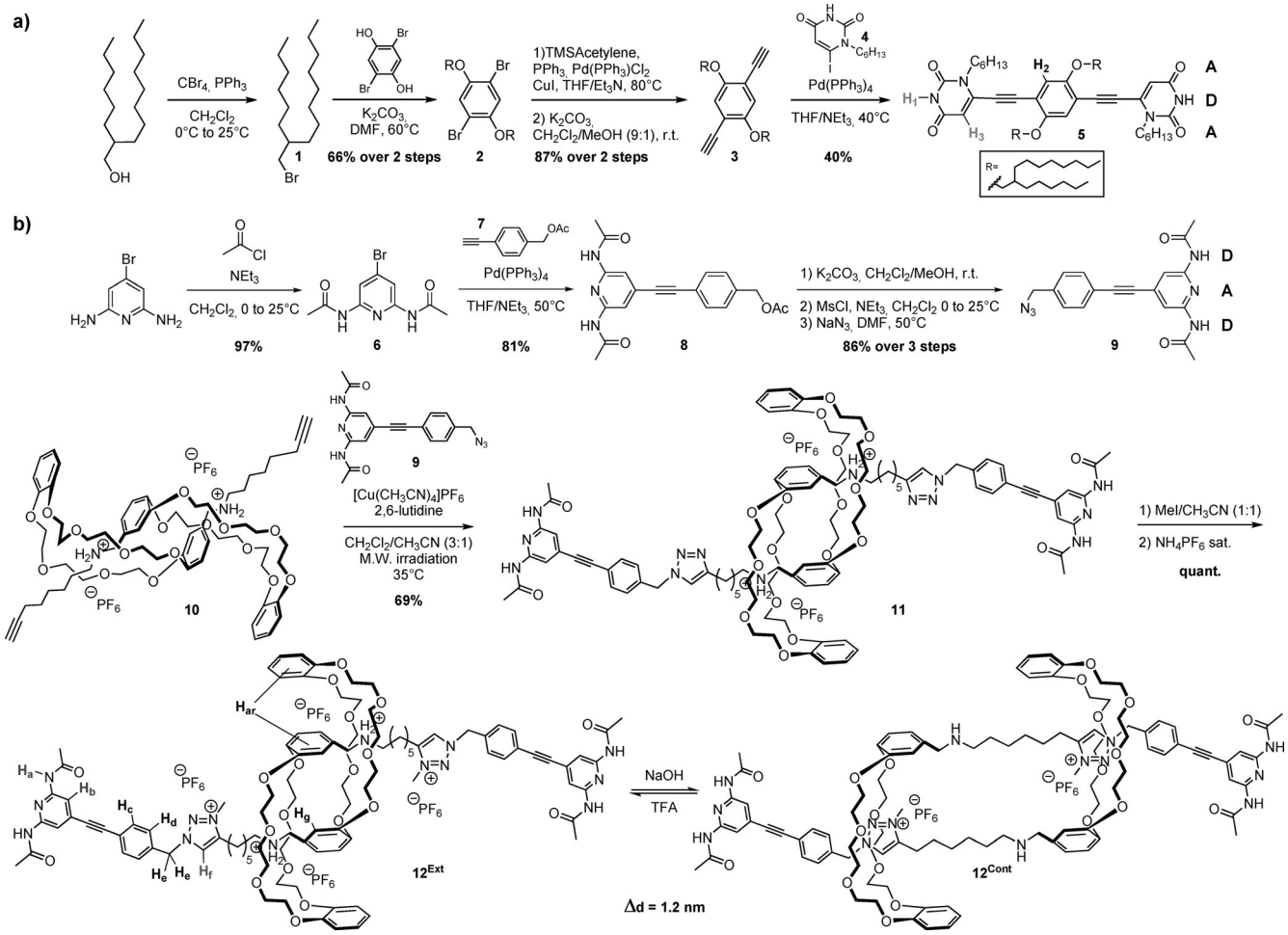

Scheme 1. a) Synthesis of bis(uracil) linker **5**. b) Synthesis of [*c*2]daisy-chain rotaxanes $\mathbf{12}^{\mathbf{Ext}}$ and $\mathbf{12}^{\mathbf{Cont}}$ with 2,6-diacetylamino pyridine stoppers.

reacted with 2,5-dibromohydroquinone to yield bis(ether) **2**. Then, a first Sonogashira coupling with trimethylsilylacetylene followed by deprotection of the TMS (trimethylsilyl) groups under basic conditions yielded bis(alkyne) **3** in excellent yield. This molecule was finally coupled with 1-hexyl-6-iodouracil **4** (prepared by procedures from the literature)[20] using another copper-free Sonogashira reaction to yield bis(uracil) linker **5** with an ADA (acceptor–donor–acceptor) hydrogen-bond pattern. On the other hand (Scheme 1 b), rotaxane $\mathbf{12}^{\mathbf{Ext}}$ was obtained in seven steps from commercially available 4-bromo-2,6-diaminopyridine, which was first acylated using acetyl chloride to yield the complementary DAD (donor–acceptor–donor) hydrogen-bond unit **6**. This compound was then coupled under copper-free Sonogashira conditions with alkyne **7**[10] to provide derivative **8** in good yield. Successive saponification of the acetate under mild conditions, activation of the resulting free alcohol with methanesulfonyl chloride, and substitution of the mesylate by sodium azide afforded DAD azide **9** (> 800 mg). This azide was then engaged in a copper-catalyzed Huisgen 1,3-dipolar cycloaddition reaction with pseudo-rotaxane **10**[21,22] under microwave activation to afford [*c*2]daisy chain rotaxane **11** in good yield and only two hours (instead of several days by classical heating). Further methylation of the triazole units of **11** yielded compound $\mathbf{12}^{\mathbf{Ext}}$ quantitatively, which could be deprotonated using a 1 M NaOH solution to provide rotaxane $\mathbf{12}^{\mathbf{Cont}}$.

The contraction/extension event associated with compound **12** was characterized by ^{1}H NMR spectroscopy at a concentration of 10^{-3} M in a 4:1 mixture of $CDCl_3/CD_3CN$ (Figure 1 a). As reported previously for other [*c*2]daisy chain rotaxanes, ^{1}H NMR spectra of $\mathbf{12}^{\mathbf{Ext}}$ and $\mathbf{12}^{\mathbf{Cont}}$ correspond to mixtures of diastereoisomers.[10,21,23] In the extended protonated state ($\mathbf{12}^{\mathbf{Ext}}$), the affinity of the electron-rich crown ether is higher for the electron-poor secondary ammonium than for the triazolium, and proton H_f of the triazole ring displays a characteristic resonance signal at 7.81 ppm. Upon deprotonation, the crown ether does not complex anymore the deprotonated secondary amine and thus slides to the triazolium cation, resulting in a contraction of the molecule toward $\mathbf{12}^{\mathbf{Cont}}$. This event is confirmed by i) the shift downfield of the triazolium proton signal H_f, moving from 7.81 ppm ($\mathbf{12}^{\mathbf{Ext}}$) to 8.92 ppm ($\mathbf{12}^{\mathbf{Cont}}$) and ii) the broadening and downfield shifts of benzylic proton H_e and aromatic protons H_d located close to the triazolium units (Figure 1 a). Importantly, the reversibility of this contraction was confirmed by adding two equivalents of deuterated trifluoroacetic acid (Figure S4). Further exchange of the counter ions using a saturated

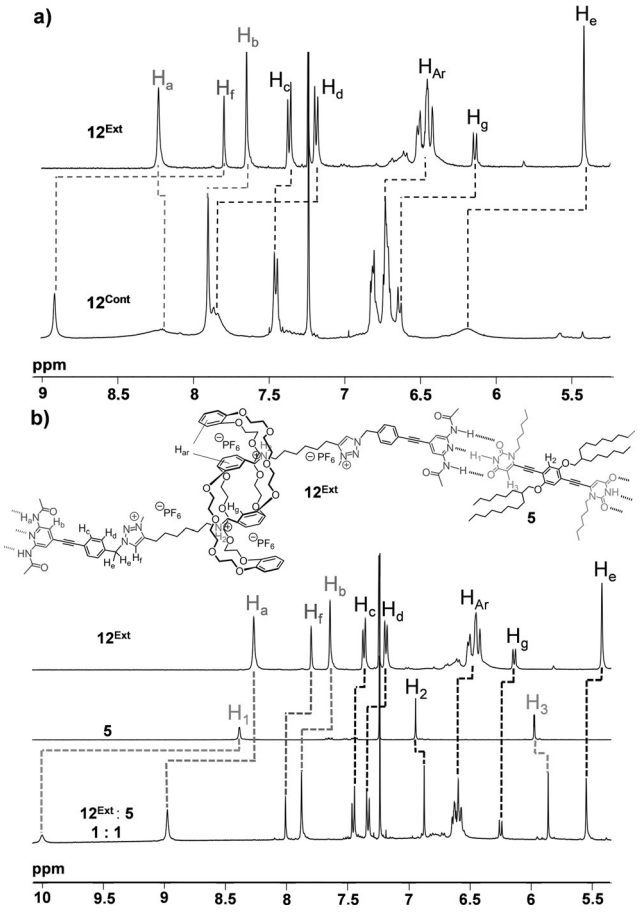

Figure 1. a) ^{1}H NMR spectra of monomers $\mathbf{12^{Ext}}$ and $\mathbf{12^{Cont}}$ in a 4:1 mixture of $CDCl_3/CD_3CN$. b) ^{1}H NMR spectrum of supramolecular polymer $\mathbf{12^{Ext}}$:**5** obtained from the 1:1 association of $\mathbf{12^{Ext}}$ and linker **5** in a 4:1 mixture of $CDCl_3/CD_3CN$.

aqueous solution of NH_4PF_6 yielded a ^{1}H NMR spectrum similar to the one of initial rotaxane $\mathbf{12^{Ext}}$.

Compound $\mathbf{12^{Ext}}$ was then mixed in a 1:1 ratio with complementary linker **5** in order to form the corresponding hydrogen-bonded supramolecular complex $\mathbf{12^{Ext}}$:**5**. In a 4:1 mixture of $CDCl_3/CD_3CN$ and at a concentration of 10^{-3} M, ^{1}H NMR spectrum displays the characteristic features of supramolecular association as protons NH_a and NH_1 are markedly shifted downfield, a typical signature for this hydrogen-bonding pattern (Figure 1 b). Similar spectroscopic observations were made when linker **5** was mixed in a 1:1 ratio with rotaxane $\mathbf{12^{Cont}}$ in a 4:1 mixture of $CDCl_3/CD_3CN$ at 10^{-3} M, confirming the formation of supramolecular complex $\mathbf{12^{Cont}}$:**5** (Figure S7b). When ^{1}H NMR spectra of $\mathbf{12^{Ext}}$:**5** and $\mathbf{12^{Cont}}$:**5** were recorded at concentrations higher than 4×10^{-3} M, an important broadening of the signals was observed (Figure S8), probably indicating the growth and the overlapping of polymer chains at this concentration.

To probe at a larger scale the formation of these supramolecular polymers in solution, we further combined static light scattering (SLS) and small-angle neutron scattering (SANS) experiments, which provide information in the range of 1–300 nm (see section 5 and Figure S9 in the Supporting Information). Investigations were performed on 4×10^{-3} M solutions at which interchain aggregation of the polymer was suspected by ^{1}H NMR spectroscopy. Qualitatively, for scattering vectors q ranging between 7×10^{-4} and 3×10^{-3} Å^{-1}, a pronounced increase in scattering intensity was observed, confirming the formation of aggregates larger than 200 nm, as no low-q Guinier regime associated to the finite size of the scattered objects is observed. The different slopes in these two experiments also indicate that a structural change occurs upon mechanical contraction/extension of the rotaxane, going from smooth two-dimensional objects $\mathbf{12^{Ext}}$:**5** (q^{-2} slope) to three-dimensional assemblies with a rough interface for $\mathbf{12^{Cont}}$:**5** (q^{-3} slope). For q higher than 4×10^{-3} Å^{-1}, both solutions are similar and display only very low and almost flat diffusion over the whole q- range accessible by SANS. This observation highlights the formation of very dense aggregates, the internal structure of which could unfortunately not be determined. Thus, and although scattering experiments cannot be used to determine the full structural parameters of these polymers, they indicate the formation of large, dense, but different self-assembled structures for $\mathbf{12^{Ext}}$:**5** and $\mathbf{12^{Cont}}$:**5** in solution.

To further determine the morphology of these supramolecular polymers, we performed imaging experiments, namely transmission electron microscopy (TEM) and atomic force microscopy (AFM). When prepared from solutions at a concentration lower than 4×10^{-3} M, monomers **5**, $\mathbf{12^{Ext}}$, and $\mathbf{12^{Cont}}$ and corresponding polymers $\mathbf{12^{Ext}}$:**5** and $\mathbf{12^{Cont}}$:**5** did not show large supramolecular organization or self-assembled architectures. However, for an initial concentration equal or higher than 4×10^{-3} M, each one of the two polymers displayed a particular mesostructure (Figure 2), while monomers still did not show any kind of structuration. Thus, the formation of such large objects results from the cooperative main-chain supramolecular polymerization afforded by the hydrogen-bond recognition pattern together with the reinforcing lateral aggregations afforded by the rigid linkers. By drop-casting the solution of $\mathbf{12^{Ext}}$:**5**, uniform structures of relatively soft entangled fibers with extended lengths of several micrometers were revealed by TEM and AFM (Figure 2 b,d). AFM experiments further detailed that these micrometric fibers arise from the lateral aggregation of fibrils having a width of 3 nm (Figures 2 f and S10). Molecular modeling confirms that such a diameter corresponds to a single chain of hydrogen-bonded polymers (see section 8 in the Supporting Information). In a hierarchical structuring, these single chains further bundle into wider fibers with a diameter ranging from 10 to 20 nm. By comparison with previously reported single-chain polyrotaxanes,[10] one may conclude that the supplementary lateral aggregation arises mainly from additional non-covalent interactions because of the presence of linker **5**, namely by π–π stacking and van der Waals interactions. Along the same lines, additional AFM imaging of neutral triazole-based **11**:**5** polymer (1:1 ratio) under similar conditions (4:1 mixture of $CHCl_3/CH_3CN$ at 4×10^{-3} M) also demonstrated the formation of closely related supramolecular architectures, thus discarding a major influence of electrostatic interactions, which would originate from the triazolium units, in the bundling process. Interestingly, for

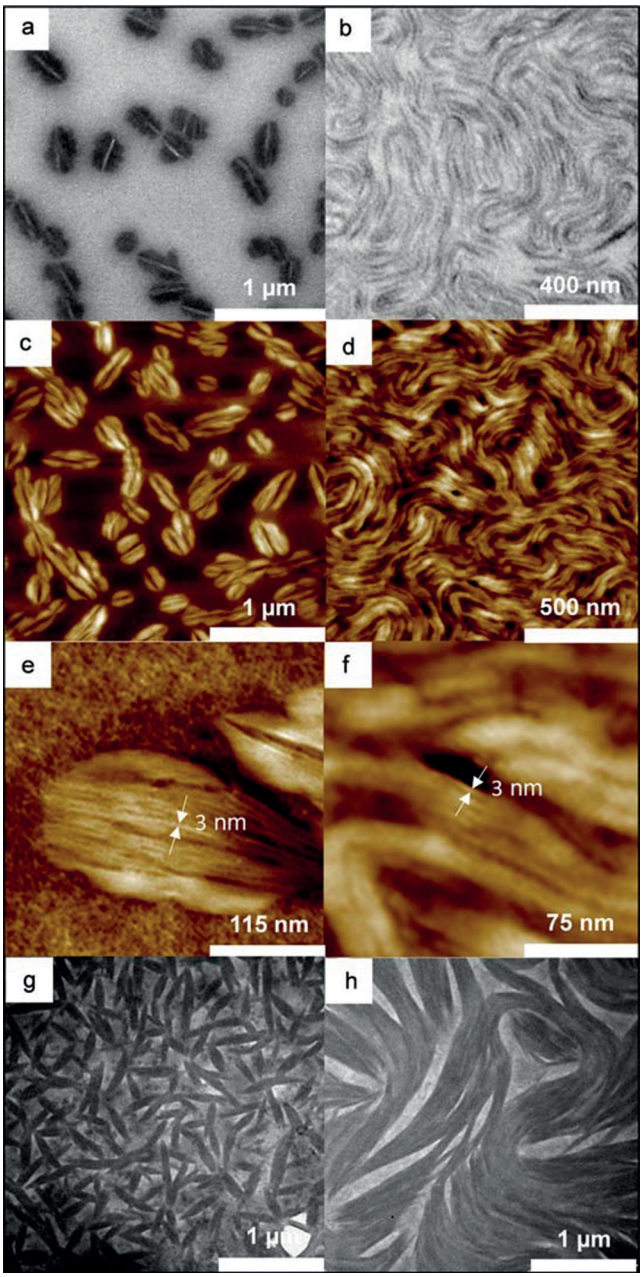

Figure 2. a,b) TEM images of supramolecular polymers a) $\mathbf{12}^{\mathbf{Cont}}$:**5** and b) $\mathbf{12}^{\mathbf{Ext}}$:**5** after drop-casting a 4×10^{-3} M solution in a 4:1 mixture of $CHCl_3/CH_3CN$ on a TEM grid. c–f) AFM topography images of polymers c,e) $\mathbf{12}^{\mathbf{Cont}}$:**5** and d,f) $\mathbf{12}^{\mathbf{Ext}}$:**5** directly scanned from the grids prepared for TEM experiments. g,h) TEM images of g) in situ contraction of supramolecular polymer $\mathbf{12}^{\mathbf{Ext}}$:**5** upon addition of two equivalents of DABCO and h) in situ extension of $\mathbf{12}^{\mathbf{Cont}}$:**5** upon addition of two equivalents of trifluoroacetic acid.

$\mathbf{12}^{\mathbf{Cont}}$:**5**, TEM and AFM analyses revealed the formation of very different mesoscale morphologies. Discrete objects were imaged, with smaller lengths comprised between 200 and 400 nm (Figure 2a,c). Additionally, the local probing of these more rigid objects by high-resolution AFM revealed that their internal structure is also built on the lateral aggregation of about three-nanometer-thick single chain polymers (Figure 2e), still in agreement with molecular modeling (see section 8 in the Supporting Information). These microscopy experiments also match with scattering data, suggesting that morphologies observed on surface are highly similar to the ones already present in solution. Furthermore, the differences of morphologies observed by microscopies for the extended and contracted polymers can be confidently correlated to the global actuation of the individual mechanical bonds. Indeed, according to our previous work, to present molecular modeling (see section 8), and to related theoretical studies,[10,24] the length of the [*c*2]daisy chain rotaxanes should here change by about 1.2 to 1.6 nm. Because of the double-threaded rotaxane configuration, one can notice a limited degree of flexibility and a higher rigidity of the polymer chain when the crown ethers are located around the triazolium units. This telescopic contraction is also intended to decrease the lateral association between the main chains by providing a higher steric hindrance in the proximity of monomer **5**. Thus, the length of the single chains can be affected directly by the actuation of the mechanical bond, but also by the change in lateral aggregation because of cooperative effects, in agreement with microscopic observations. Finally, imaging experiments from in situ extension and contraction of the polymer chains in solution confirmed the overall trend in the actuation of the system and its morphological transition by integrated dynamic motions (Figures 2g,h). The in situ contraction of $\mathbf{12}^{\mathbf{Ext}}$:**5** using two equivalents of 1,4-diazabicyclo[2.2.2]octane (DABCO) yielded smaller and more rigid structures, with sizes comprised between 200–500 nm (Figure 2g). The in situ extension of $\mathbf{12}^{\mathbf{Cont}}$:**5** using two equivalents of trifluoroacetic acid (TFA) yielded soft entangled fiber structures of several micrometers long (Figure 2h).

In conclusion, we have designed and synthesized the first examples of muscle-like hydrogen-bonded supramolecular polymers. They involve a [*c*2]daisy chain rotaxane decorated with 2,6-diacetylamino pyridine stoppers and a complementary bis(uracil) linker. In organic solvents, a hierarchical association upon increasing concentration leads to large bundles of fibers, as confirmed by NMR spectroscopy, light and neutron scattering in solution, and microscopy techniques. Importantly, we have shown that a local actuation between extended and contracted rotaxanes gives rise to morphological variations of the self-assemblies at mesoscale. These experiments demonstrate the possibility to bundle single-chain contractile supramolecular polymers into stiffer fibers, and to integrate thousands of molecular machines over switchable hierarchical mesostructures. This work represents an important step towards understanding the amplification of molecular motions at higher length scales, and for ultimately targeting artificial muscle-like materials using bottom-up approaches.

Acknowledgements

The research leading to these results has received funding from the European Research Council under the European Community's Seventh Framework Program (FP7/2007-2013, agreement number 257099). We wish to thank the CNRS, the COST action CM 1304, the international center for Frontier

Research in Chemistry, the Laboratory of Excellence for Complex System Chemistry, the University of Strasbourg, the University of Paris Diderot (Sorbonne Paris Cité), and the Institut Universitaire de France (N.G.) for financial supports. This work was also supported by the Agence Nationale pour la Recherche (grant number ANR-14-CE06-0021), the French Ministry of Research (fellowship to A.G.) and the China Scholarship Council (fellowship to G.D.). We also wish to thank the Laboratoire Léon Brilloin (LLB, CEA, Saclay, France) for beamtime allocation and Dr. J. M. Strub for high-resolution mass spectroscopic experiments.

Keywords: molecular machines · nanotechnology · rotaxanes · soft matter · supramolecular polymers

How to cite: *Angew. Chem. Int. Ed.* **2016**, *55*, 703 – 707
Angew. Chem. **2016**, *128*, 713 – 717

[1] K. Kinbara, T. Aida, *Chem. Rev.* **2005**, *105*, 1377 – 1400.
[2] M. Schliwa, G. Woehlke, *Nature* **2003**, *422*, 759 – 765.
[3] J. L. Krans, *Nat. Educ.* **2010**, *3*, 66 – 69.
[4] a) C. J. Bruns, J. F. Stoddart, *Acc. Chem. Res.* **2014**, *47*, 2186 – 2199; b) A. Coskun, M. Banaszak, R. D. Atsumian, J. F. Stoddart, B. A. Grzybowski, *Chem. Soc. Rev.* **2012**, *41*, 19 – 30.
[5] Q. Li, G. Fuks, E. Moulin, M. Maaloum, M. Rawiso, I. Kulic, J. T. Foy, N. Giuseppone, *Nat. Nanotechnol.* **2015**, *10*, 161 – 165.
[6] W. R. Browne, B. L. Feringa, *Nat. Nanotechnol.* **2006**, *1*, 25 – 35.
[7] M. Jiménez, C. Dietrich-Buchecker, J. Sauvage, *Angew. Chem. Int. Ed.* **2000**, *39*, 3284 – 3287; *Angew. Chem.* **2000**, *112*, 3422 – 3425.
[8] L. Fang, M. Hmadeh, J. Wu, M. A. Olson, J. M. Spruell, A. Trabolsi, Y. W. Yang, M. Elhabiri, A. M. Albrecht-Gary, J. F. Stoddart, *J. Am. Chem. Soc.* **2009**, *131*, 7126 – 7134.
[9] P. G. Clark, M. W. Day, R. H. Grubbs, *J. Am. Chem. Soc.* **2009**, *131*, 13631 – 13633.
[10] G. Du, E. Moulin, N. Jouault, E. Buhler, N. Giuseppone, *Angew. Chem. Int. Ed.* **2012**, *51*, 12504 – 12508; *Angew. Chem.* **2012**, *124*, 12672 – 12676.
[11] L. Gao, Z. Zhang, B. Zheng, F. Huang, *Polym. Chem.* **2014**, *5*, 5734 – 5739.
[12] D. González-Rodríguez, A. P. H. J. Schenning, *Chem. Mater.* **2011**, *23*, 310 – 325.
[13] F. H. Beijer, R. P. Sijbesma, J. A. J. M. Vekemans, E. W. Meijer, H. Kooijman, A. L. Spek, *J. Org. Chem.* **1996**, *61*, 6371 – 6380.
[14] C. Fouquey, J.-M. Lehn, A.-M. Levelut, *Adv. Mater.* **1990**, *2*, 254 – 257.
[15] T. Gulik-Krzywicki, C. Fouquey, J. Lehn, *Proc. Natl. Acad. Sci. USA* **1993**, *90*, 163 – 167.
[16] L. Đorđević, T. Marangoni, T. Miletić, J. Rubio-Magnieto, J. Mohanraj, H. Amenitsch, D. Pasini, N. Liaros, S. Couris, N. Armaroli, M. Surin, D. Bonifazi, *J. Am. Chem. Soc.* **2015**, *137*, 8150 – 8160.
[17] A. Wolf, E. Moulin, J. J. Cid Martín, A. Goujon, G. Du, E. Busseron, G. Fuks, N. Giuseppone, *Chem. Commun.* **2015**, *51*, 4212 – 4215.
[18] K. Yoosaf, A. Llanes-Pallas, T. Marangoni, A. Belbakra, R. Marega, E. Botek, B. Champagne, D. Bonifazi, N. Armaroli, *Chem. Eur. J.* **2011**, *17*, 3262 – 3273.
[19] A. Llanes-Pallas, M. Matena, T. Jung, M. Prato, M. Stöhr, D. Bonifazi, *Angew. Chem. Int. Ed.* **2008**, *47*, 7726 – 7730; *Angew. Chem.* **2008**, *120*, 7840 – 7844.
[20] A. Llanes-Pallas, C. A. Palma, L. Piot, A. Belbakra, A. Listorti, M. Prato, P. Samorì, N. Armaroli, D. Bonifazi, *J. Am. Chem. Soc.* **2009**, *131*, 509 – 520.
[21] F. Coutrot, C. Romuald, E. Busseron, *Org. Lett.* **2008**, *10*, 3741 – 3744.
[22] F. Coutrot, *ChemistryOpen* **2015**, DOI: 10.1002/open.201500088.
[23] S. J. Cantrill, G. J. Youn, J. F. Stoddart, D. J. Williams, *J. Org. Chem.* **2001**, *66*, 6857 – 6872.
[24] Y.-L. Zhao, R.-Q. Zhang, C. Minot, K. Hermann, M. A. Van Hove, *Phys. Chem. Chem. Phys.* **2015**, *17*, 18318 – 18326.

Received: October 20, 2015
Published online: November 19, 2015

